# Undulator Radiation and Free-Electron Lasers as X-ray Sources

Sheena Patel (skkpatel@physics.ucsd.edu)

Phys239: Radiative Processes in Astrophysics
November 30, 2016

**Abstract**

For several decades now, synchrotron radiation sources have been the most powerful X-ray sources for the study of physical properties of matter. More recently, however, undulator radiation has allowed for the development of free-electron laser X-ray sources with higher intensity and advantages such as monochromatic energy spectra and femtosecond pulses. Undulator radiation is the radiation that is emitted as electrons oscillate in a plane through an undulator, a series of alternating dipole magnets. The radiation emitted is concentrated in a narrow cone around the electron path axis. Free-electron lasers such as the Linac Coherent Light Source at SLAC National Accelerator Laboratory use this undulator radiation to provide high intensity X-ray beams with ultrafast pulses.

## 1 Introduction

Today in experimental condensed matter physics, X-rays are one of the most powerful tools in measuring various properties of materials and devices. Many of the X-ray techniques are implemented in synchrotron facilities, making use of the synchrotron radiation that is emitted from electrons traveling in a circular path. At these facilities, there is a large storage ring, usually somewhere around 1 km in diameter, in which electron bunches travel in a circular path, emitting X-rays. "Beamlines" are set up around the storage ring tangential to the path of the electrons to use the X-ray emission beam for various experiments. These facilities have provided a profound improvement to the X-ray methods that were available previously, primarily because the X-ray intensities available in these synchrotron facilities are several orders of magnitude higher than those in standard X-ray tubes [1].

More recently, though, the development of the free-electron laser has provided another huge improvement in the X-ray source technology. These free-electron lasers are made up to two components: an accelerator that provides a bunched beam of electrons traveling at relativistic speeds and an undulator, which is a linear series of alternating dipole magnets. Electrons traveling in this undulator follow a roughly sinusoidal path, during which they emit X-rays (or undulator radiation). This undulator radiation from free-electron lasers has intensity around eight orders of magnitude

higher than that of the radiation in synchrotron facilities and allows for X-ray coherence and femtosecond scale pulses, providing a very powerful tool in probing material properties and physical phenomena [1, 2].

There are still far fewer free-electron lasers in use compared to synchrotron facilities. Free-electron lasers are a newer concept and the linear electron and X-ray paths allow for only one (or two by making use of a beam-splitter) experiment at a time, whereas synchrotrons can make use of many lines of X-rays tangential to the electron storage ring. One of the free-electron laser facilities in the United States that is available to submit proposals for X-ray measurements is the Linac Coherent Light Source (LCLS) at SLAC National Accelerator Laboratory. LCLS has been the source of many interesting insights into condensed matter phenomena [1, 2].

## 2 Electron Motion in an Undulator

An undulator with the resulting electron motion is shown schematically in Fig. 1. The undulator is two very long series of alternating dipole magnets with orientations as shown and separated from adjacent magnets by magnet pole shoes (pieces of iron usually). Each pair of magnets, one up and one down, is about 25 mm horizontally. Between the two series of magnets, an electron that is traveling horizontally, parallel to the magnets, oscillates in the horizontal plane as a result of the fields with a deflection of a few μm [1]. In Fig. 1b, a top view of the undulator is shown with the electron path overlaid.

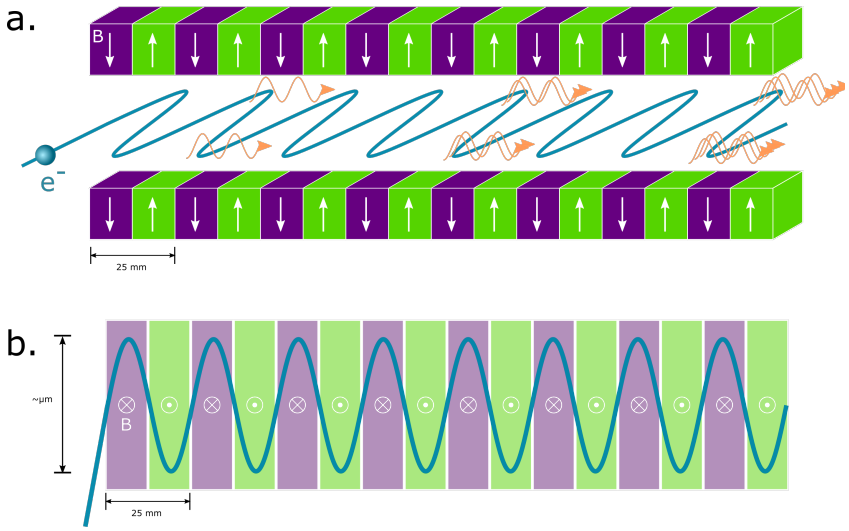


Figure 1: Schematic of electron motion in an undulator. (a) A series of alternating vertical dipole magnets (with thin magnet pole shoes between them) form an undulator. In the presence of this kind of alternating magnetic field, a charged particle (here, an electron) will be deflected by the field so that it oscillates in the horizontal plane with an amplitude of a few μm over a period of 25 mm. The constant acceleration results in the emission of radiation. (b) A top view of the electron motion overlaid with the dipole magnet directions.

When traversing this path, the electron is constantly accelerating. This results in what is referred to as undulator radiation. To describe the electron's path, let's first take the axis of the undulator along the beam direction to be the $z$-axis with magnetic field in the $+y$- and $-y$-directions. Let the period of the magnet arrangement and therefore the period of the oscillations, be $\lambda_u$, usually around 20-30 mm,. If the $x$-width of the magnets is much larger than $\lambda_u$, we can assume no $x$-dependence of the field in the electron path. The divergence of the magnetic field vanishes so we can write it as a gradient of a scalar magnetic potential $\phi_{\text{mag}}$ that obeys the Laplace equation: $\boldsymbol{B} = -\boldsymbol{\nabla}\phi_{\text{mag}}$, $\boldsymbol{\nabla}^2\phi_{\text{mag}} = 0$. This potential can be approximated as $\phi_{\text{mag}}(y,z) = f(y)\sin(k_u z)$ where $k_u = 2\pi/\lambda_u$. Since $\frac{d^2 f}{dy^2} - k_u^2 f = 0$, we obtain the general solution $\phi_{\text{mag}} = (c_1 \sinh(k_u y) + c_2 \cosh(k_u y))\sin(k_u z)$. From this, we can obtain $B_y(y,z) = -\frac{\partial \phi_{\text{mag}}}{\partial y}$, apply symmetry conditions, and let $B_0 = k_u c_1$ to see that $c_2 = 0$ and get solutions of

$$\phi_{\text{mag}}(x,y,z) = \frac{B_0}{k_u}\sinh(k_u y)\sin(k_u z)$$

$$\begin{aligned} B_x &= 0 \\ B_y &= -B_0 \cosh(k_u y)\sin(k_u z) \\ B_z &= -B_0 \sinh(k_u y)\cos(k_u z) \end{aligned}$$

Since we are limiting our electron is moving only in the $x-z$ plane, we can assume $y = 0$ and use $\boldsymbol{B} = -B_0 \sin(k_u z)\hat{\boldsymbol{y}}$ [1].

The total relativistic energy of the electron can be expressed as $\gamma m_e c^2$. The transverse acceleration, a result of the Lorentz force in the presence of the magnetic field, is $\gamma m_e \dot{\boldsymbol{v}} = -e\boldsymbol{v} \times \boldsymbol{B}$, which gives us $\ddot{x} = \frac{e}{\gamma m_e} B_y \dot{z}$ and $\ddot{z} = -\frac{e}{\gamma m_e} B_y \dot{x}$. To first-order, we see that $\dot{z} \approx v = \beta c \approx$ const and $\dot{x} \ll \dot{z}$. This gives us $x(t) \approx \frac{eB_0}{\gamma m_e \beta c k_u^2}\sin(k_u \beta c t)$ and $z(t) \approx \beta c t$. With the initial conditions $x(0) = 0$ and $\dot{x}(0) = \frac{eB_0}{\gamma m_e k_u}$, we get a sinusoidal trajectory

$$x(z) = \frac{K}{\beta\gamma k_u}\sin(k_u z)$$

where

$$K = \frac{eB_0}{m_e c k_u} = \frac{eB_0\lambda_u}{2\pi m_e c} = 0.934 \cdot \frac{B_0}{[\text{T}]} \cdot \frac{\lambda_u}{[\text{cm}]}$$

is the dimensionless undulator parameter [1].

To second order, the assumption that $\dot{z} = 0$ is false because of the deflection of the electron in the $x$ direction. The $z$-velocity is instead $\dot{z} = \sqrt{v^2 - \dot{x}^2} \approx c\left(1 - \frac{1}{2\gamma^2}(1 + \gamma^2 \dot{x}^2/c^2)\right)$. By inserting the first order solution for $\dot{x}$, we get

$$v_z(t) = \left(1 - \frac{1}{2\gamma^2}\left(1 + \frac{K^2}{2}\right)\right)c - \frac{cK^2}{4\gamma^2}\cos(2\omega_u t)$$

So to second order, the electron path is given by

$$x(t) = \frac{K}{\gamma k_u} \sin \omega_u t$$
$$z(t) = \bar{v}_z t - \frac{K^2}{8\gamma^2 k_u} \sin(2\omega_u t)$$

where the average longitudinal speed is $\bar{v}_z = \left(1 - \frac{1}{2\gamma^2}\left(1 + \frac{K^2}{2}\right)\right) c \equiv \bar{\beta} c$ [1].

# 3 Radiation from Electrons in an Undulator

Since an electron's deflection in an undulator is purely because of a perpendicular force due to the magnetic field, the radiation will instantaneously be emitted tangentially just like with synchrotron radiation from a circular path. The difference is that the small amplitude results in a narrow cone of radiation with a maximum angle with respect to the $z$-axis of $\theta_{\text{max}} \approx \left|\frac{dx}{dz}\right|_{\text{max}} = \frac{K}{\beta\gamma} \approx \frac{K}{\gamma}$. For small $K$ values, up to 2 or 3, there is an important consequence: the radiation emitted from the electrons at various points in space interferes such that the radiation spectrum is a narrow spectral line at a well-defined frequency and its odd higher harmonics, so the radiation is nearly monochromatic [1].

First, we con consider the radiation in a coordinate system moving with the average $z$-velocity of the electrons, $\bar{v}_z$. The Lorentz transformation to this system is

$$t^* = \bar{\gamma}(t - \bar{\beta} z/c) \approx \bar{\gamma} t(1 - \bar{\beta}^2) = \frac{t}{\bar{\gamma}}$$
$$x^* = x = \frac{K}{\gamma k_u} \sin(\omega_u t)$$
$$z^* = \bar{\gamma}(z - \bar{\beta} c t) \approx -\frac{K^2}{8\gamma k_u \sqrt{1 + K^2/2}} \sin(2\omega_u t)$$

In this coordinate system, the electron can be considered an oscillating dipole moving at non-relativistic speeds, so the Larmor formula of power radiated from an electric charge $P = \frac{e^2}{6\pi\varepsilon_0 c^3} \dot{\boldsymbol{v}}^2$ is valid. Ignoring the smaller longitudinal oscillation component, the acceleration can be approximated as $\dot{v}_{x^*} = \frac{d^2 x^*}{dt^{*2}} = -\frac{K\gamma c^2 k_u}{1 + K^2/2} \sin(\omega_u t)$. By time-averaging this acceleration, we have a total radiated power in the moving coordinate system of $P^* = \frac{e^2 c \gamma^2 K^2 k_u^2}{12\pi\varepsilon_0 (1 + K^2/2)^2}$. Transforming back into laboratory coordinates gives us the same total radiated power per electron $P = P^*$. This power ignores the contribution from the longitudinal oscillation, which adds contributions to higher odd harmonics. The total power of undulator radiation summed over all harmonics and angles is equivalent to the synchrotron radiation power in a magnetic field of $B = B_0/\sqrt{2}$:

$$P_{\text{rad}} = \frac{e^4 \gamma^2 B_0^2}{12\pi\varepsilon_0 c m_e^2} = \frac{e^2 c \gamma^2 K_2 k_u^2}{12\pi\varepsilon_0}$$

However, the spatial distribution of the power changes significantly when we move back into the laboratory frame, as shown in Fig. 2: the emitted power is concentrated in the forward direction in

the laboratory frame [1].

In the rest frame, the electron acts as a dipole oscillating in the $x^*$ direction with equivalent spatial power emission in the $+z$- and $-z$-directions. In a frame where the electron is moving in the $+z$-direction, the radiation is more concentrated in the forward direction, resulting in a distribution as in Fig. 2b. [1].

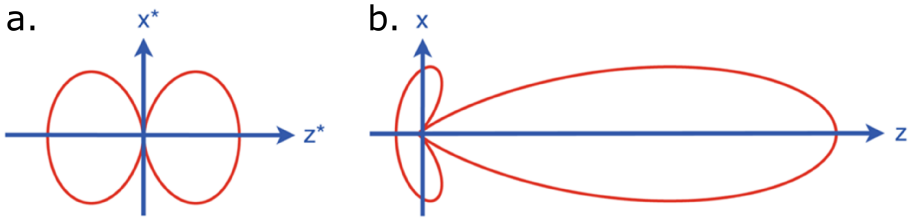


Figure 2: Spatial distribution from a dipole (a) oscillating in the $x^*$-direction and at rest in the $z^*$-direction or (b) oscillating in the $x$-direction and moving in the $z$-direction with speed $v_z = 0.9c$. Fig. from [1].

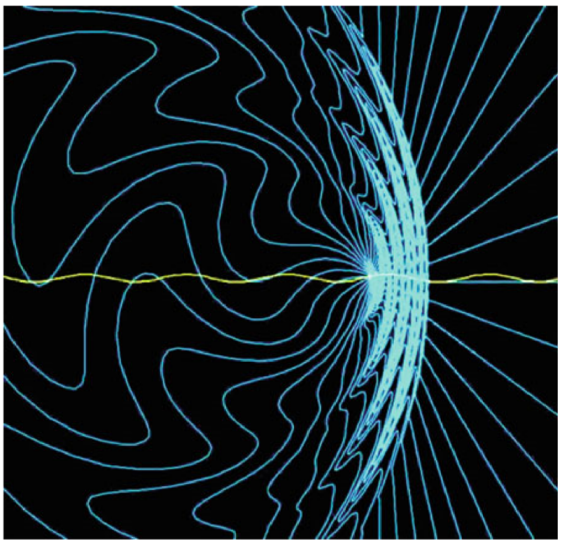

Figure 3: A numeric calculation of the field lines of the undulator radiation from an electron with $v = 0.9c$ and undulator parameter $K = 1$. The yellow line shows the electron trajectory in the undulator. Fig. from [1].

The radiated energy in the moving coordinate frame as a function of the emission angle $\theta$ is $\hbar\omega^* = \bar{\gamma}(W_{\text{ph}} - \bar{\beta}cp_{\text{ph}}\cos\theta) = \bar{\gamma}\hbar\omega_\ell(1 - \bar{\beta}\cos\theta)$, where in the laboratory frame, $W_{\text{ph}}$ is the photon energy and $p_{\text{ph}}$ is the photon momentum. So then in the laboratory frame, the light wavelength is $\lambda_\ell = \frac{2\pi c}{\omega_\ell} \approx \omega_u(1 - \bar{\beta}\cos\theta)$. Near $\theta = 0$, the wavelength of undulator radiation is

$$\lambda_\ell(\theta) = \frac{\lambda_u}{2\gamma^2}\left(1 + \frac{K^2}{2} + \gamma^2\theta^2\right)$$

This radiation is linearly polarized with the electric vector in the $x - z$ plane of the electron path. A numeric calculation of the field lines of the undulator radiation from an electron in an undulator is shown in Fig. 3 [1]. Something of importance to notice is that the wavelength of undulator radiation can be manipulated by changing the electron energy (by changing its speed) or by changing the undulator period $\lambda_u$. This becomes useful for experimental applications when you want to probe a specific length scale [3].

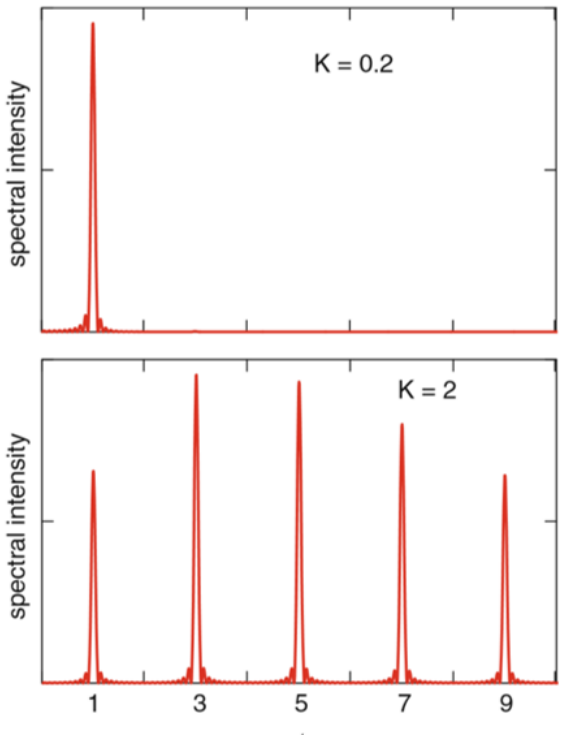


Figure 4: Spectral intensity of radiation in the forward direction from an electron in an undulator with 10 periods (near $\theta = 0$) with small undulator parameter $K = 0.2$ (top) and larger undulator parameter $K = 2$ (bottom). Fig. from [1].

One of the properties that makes the undulator so useful as an X-ray source is that its radiation consists of narrow spectral lines. Fig. 4 shows the spectral distribution for small and large undulator parameters $K$, which show narrow spectral lines and radiation at higher harmonics with larger undulator parameter [1]. The radiation is not completely monochromatic, especially as $K$ increases, but is referred to as quasi-monochromatic, with a bandwidth around 1%, which is far narrower than the broad spectral distribution from traditional synchrotron radiation. Undulator radiation also typically has a far smaller angular divergence than synchrotron radiation [2]. The coherence, monochromaticity, and small diveregence of the undulator beam provide a higher number of photons to be used in X-ray studies of materials. This also allows for a short electron bunch length to get femtosecond-scale X-ray pulses, that, for example, can be used to probe ultrafast dynamics and processes and image materials on scales that could not have been reached before [1]. Synchrotron radiation sources usually deliver pulses of 30-50 ps duration, where as free-electron

lasers can deliver pulses of 10-500 fs [6]. The advantages of undulator radiation have led to the development of free-electron laser facilities with high user demand.

# 4 Free-Electron Lasers

Each electron in a ”bunch” traveling through an undulator experiences the motion described in Section 2 and emits radiation as described in Section 3. But when we consider a bunch of electrons traveling through the undulator, the electrons also respond to the radiation field from each other electron in the bunch. This tends to modulate the electrons from one large bunch into micro-bunches which are spatially ordered with a separation equal to the X-ray wavelength. Each micro-bunch then produces radiation that is in phase with the radiation from all the other micro-bunches. The radiation field increases rapidly along the undulator and the micro-bunching and radiation production will enhance itself through Self-Amplified Stimulated Emission (SASE) [2].

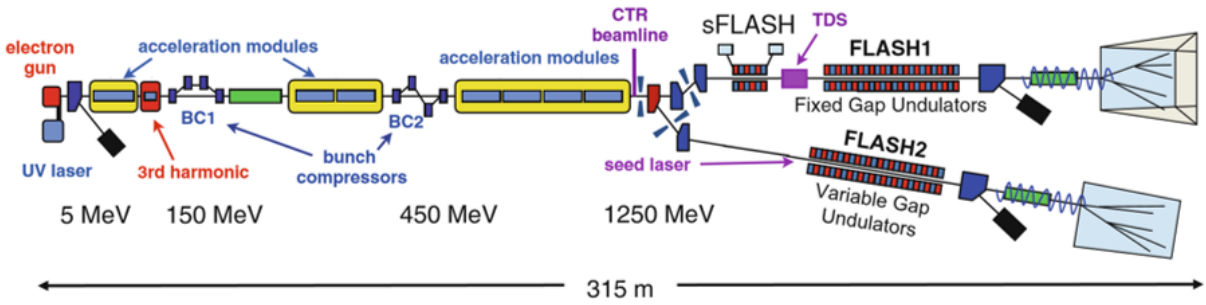


Figure 5: Schematic of the free-electron laser FLASH (Free-Electon Laser in Hamburg). Electron bunches are produced in a photo-injector and accelerated in a superconducting linear accelerator up to energies as high as 1250 MeV with acceleration modules and bunch compressors. The total bunch charge is around 0.1 to 0.5 nC. Typically, the linear setup allows for only one beamline, but here there are two beamlines operated simultaneously by sharing the bunches between the two lines. The variable gap undulator allows for changes in the undulator period and therefore the undulator parameter by manipulating $\lambda_u$ and allows tuning of the radiation to different wavelengths. Fig. from [1].

An example layout of the free-electron laser FLASH in Hamburg, Germany is shown in Fig. 5. Electron bunches, typically with total charge around a few tenths of a nC, are produced in a photo-injector (by illuminating photo-cathodes with short ultraviolet laser pulses) and accelerated in a superconducting linear accelerator to GeV energy range. Once the electrons have an appropriate energy, the beam is deflected slightly before entering the undulator in order to protect the magnets from radiation produced with the acceleration. Unlike with synchrotrons, the linear nature of undulator radiation allows for only one or two beamlines at once [1].

Fig. 6 shows the peak brilliance as a function of photon energy for some of the X-ray free-electron lasers and synchrotron facilities in existence today. The intensities of free-electron lasers are

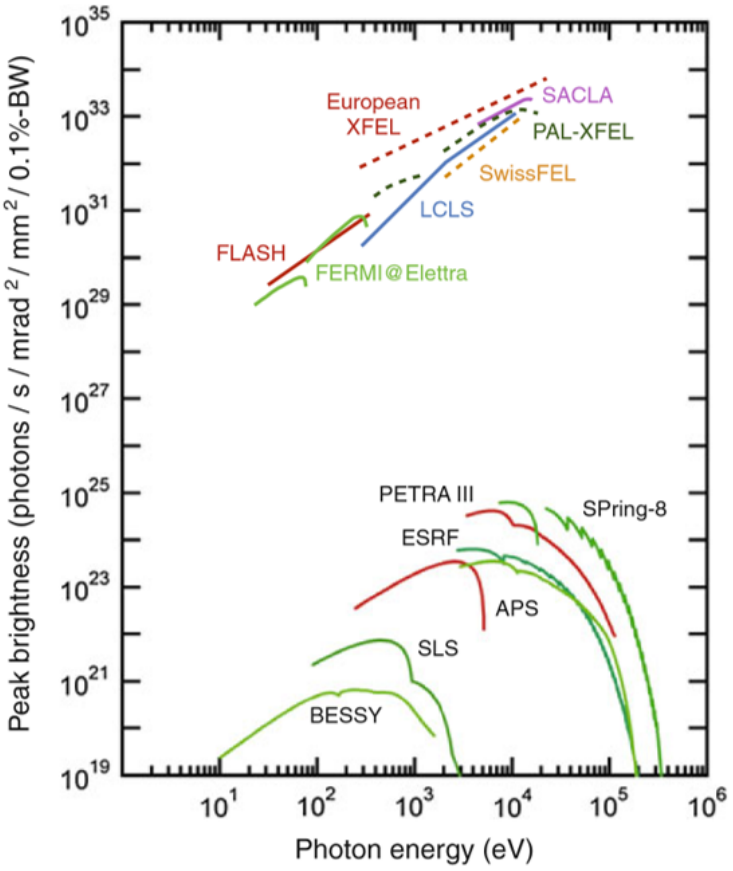


Figure 6: Peak brightness as a function of photon energy at various X-ray source facilities. The X-ray free-electron lasers are LCLS, SACLA (Japan), European XFEL (Germany), SwissFel (Switzerland), PAL-XFEL (Korea), FLASH (Germany), FERMI@Elettra (Italy). The synchrotron facilities included are APS (USA), BESSY (Germany), ESRF (France), PETRA III (Germany), SLS (Switzerland), SPring-8 (Japan). The X-ray free-electron lasers have peak brightness around eight orders of magnitude higher than the synchrotron facilities. Fig. from [1].

seven to nine orders of magnitude higher than for the synchrotron facilities. These free-electron lasers which are in operation or under construction include LCLS at Stanford in the United States, SACLA in Japan, the European XFEL in Germany,the SwissFEL in Switzerland, the PAL-XFEL in Korea, FLASH in Germany, and FERMI@Elettra in Italy. [1].

# 5 The Linac Coherent Light Source
## SLAC National Accelerator Laboratory

LCLS began operations in April 2009 as the world's first hard X-ray free-electron laser. Its peak brilliance is around ten orders of magnitude more than the brilliance from synchrotron sources such

as the Advanced Light Source (ALS) at Lawrence Berkeley National Lab (LBNL) or the Advanced Photon Source (APS) at Argonne National Lab (ANL). Fig. 7 shows some X-ray diffraction data collected at APS and LCLS (insets). The diffraction intensities were measured at about 100 points in reciprocal space at APS. This measurement took about six hours. The insets show the intensities of photons on a detector at LCLS with the setup oriented at a single value in reciprocal space. This single measurement took about half a second. If we had scanned at the same hundred points as in APS, the total measurement would have taken about one minute. This demonstrates the usefulness of the high intensity X-ray beam at LCLS [2]. In 1 fs, the LCLS X-ray beam delivers about $10^{10}$ coherent photons [6].

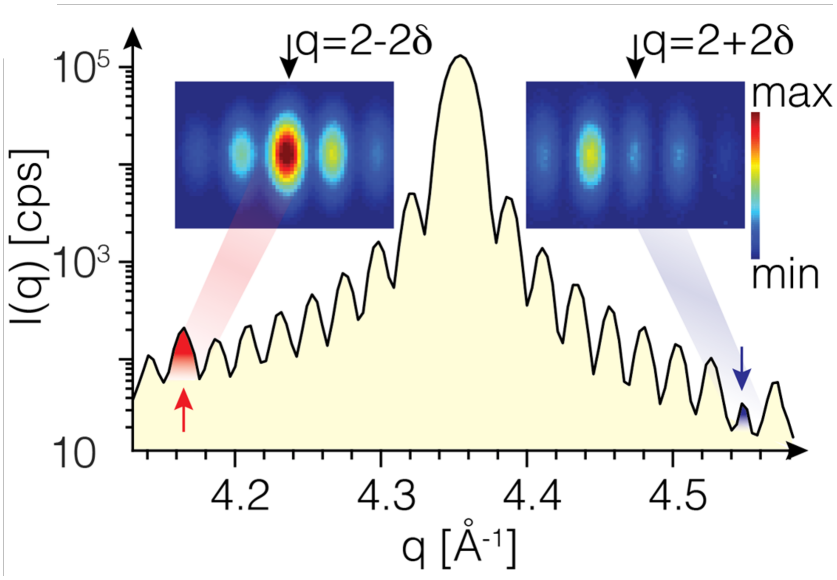


Figure 7: X-ray diffraction data taken at APS in six hours at 100 K of a thin epitaxial Cr film showing the (002) Bragg peak and Laue oscillations and the constructive (destructive) interference of the charge density wave peak below (above) the Bragg peak. The insets show a half-second count on the detector at the LCLS X-ray pump probe experiment at the positions of the charge density wave peaks. Fig. from [4].

Fig. 8 shows a schematic layout of LCLS. Electron bunches form in a copper photocathode using Ti:Sa laser (UV) pulses. The electrons are boosted to 135 MeV and then injected into the linear accelerator. This accelerator consists of the structures L0, L1, L2, and L3, which are 2.856 GHz normal-conducting traveling-wave accelerators made from copper. Along the way, the bunches are compressed in magnetic bunch compressors BC1 and BC2. The beam is deflected magnetically and collimated to protect the undulator from radiation damage from the acceleration. The undulator region consist of 33 segements of undulators, each 3.4 m in length. Each of these undulators has 1.25 T NdFeB permanent magnets with period $\lambda_u = 30$ mm and a fixed gap between the magnets of 6.8 mm. The magnet pole shoes that separate the magnets can be canted slightly to allow for some variation $\lambda_u$ and therefore in undulator parameter $K$. The achievable final electron energy can vary between 2.5 GeV and 15.8 GeV, giving an X-ray radiation wavelength range of $0.01\text{ nm} \leq \lambda_\ell \leq 4.4\text{ nm}$. The X-ray pulses are around a few mJ in energy and have a duration of

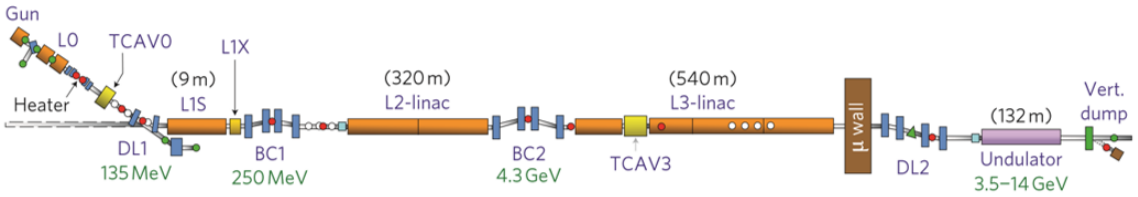


Figure 8: Schematic of the free-electron laser LCLS at SLAC National Accelerator Laboratory. Electrons are produced in a copper photocathode and boosted to 135 MeV and then injected into the linear accelerator with normal-conducting traveling-wave accelerators L0-L3 and bunch compressors BC1 and BC2. They are then deflected and enter the undulator. Fig. from [5].

10-500 fs [1, 5].

At the end of the line, past the undulators and the electron dump, LCLS has seven experiments or instruments set up for X-ray studies: Atomic, Molecular, and Optical Science (AMO), Coherent X-Ray Imaging (CXI), Matter in Extreme Conditions (MEC), Macromolecular Femtosecond Crystallography (MFX), Soft X-Ray Materials Science (SXR), X-Ray Correlation Spectroscopy (XCS), and X-Ray Pump Probe (XPP). The linear beam allows only one or two (with a beam splitter) of these instruments to be used at a time [7].

AMO experiments typically involve X-ray diffraction measurements of gasious atoms, molecules, clustors, or nanometer-scale materials like protein crystals or viruses. Electron and ion spectrometers are used to study fundamental interactions of ionizing radiation with matter, allowing insight into processes like nuclear dynamics and atomic motion to be examined at their natural time scale [7].

CXI involves X-ray diffraction to determine atomic structure of biomolecules which are destroyed through radiation damage. Here, the method used is called ”diffraction-before-destruction.” The destruction process of the molecules occurs in about 20-50 fs. At LCLS, a single short 10 fs pulse would have high enough photon count to get structural information. [6, 7].

The MEC instrument is exactly what it is called: a study of matter in extreme conditions. There is a lot ofscientific interest in studying warm dense matter, matter under high pressure, shock physics, and high energy density physics. Some of the states studied are very short-lived states, evolving on femto- and picosecond time scales. The LCLS X-ray beams allow study before this evolution and low corss-section beam with high intensity to heat homogenously to high temperatures. These are properties not available at synchrotron facilities [7].

MFC requires the high peak power and ultrashort hard X-ray pulses in the same ”diffraction-before-destruction” method as CXI, but instead of biomolecules, crystallography measurements are made on small crystals. These samples would incur structural or electronic damage with X-ray radiation. The idea is that with a short 10 fs pulse, the scattering will occur before the sample is damaged (around 20-50 fs time-frame). The X-ray intensity must be very high since only a single

pulse is possible before the sample is destroyed. The time and intensity requirements make the X-ray free-electron laser the only acceptable source for X-ray crystallography of small crystals. [7].

SXR uses soft X-rays (lower energy) for imaging or pump probe X-ray spectroscopy. This is used to understand how bonds break and form during chemical reactions. X-ray spectroxcopy allows for atom-specific probe of electronic structure. In strongly correlated materials, for example, this can beused to understante ground state properties of charge ordering and magnetic excitations. Soft X-rays are sensitive to different phenomena and particles, such as to valence electrons, so this provides a slightly different tool than the XPP setup described below. SXR also allows for magnetic imaging. A significant discovery in magnetism is the magneto-optical Kerr effect, where light will scatter slightly differently from electrons with different spins This is used to develop a 2D image of the magnetic domains or regions in a sample. [7].

When coherent light is scattered from a disordered system, the pattern of scattering in $k$-space shows a dotted or grainy pattern called "speckles," which originate from the position of the scatteres in the system. XCS studies these speckle patterns to characterize temporal fluctuations and provide insight into dynamic processes in materials [7].

The XPP experiment uses a femtosecond optical laser pulse to "pump" or generate transient states of matter and the X-ray pulses to probe structural dynamics after this pump through X-ray scattering. The laser pulse energy, frequency, and temporal profile can be manipulated to excite certain states over others in the experiment. The ultrafast X-ray pulse allows for a more precise measurement of ultrafast dynamics rather than an average over a longer X-ray pulse and higher photon counts and low beam divergence allow for measurement of thinner or smaller samples. [7].

Since 2009, these seven instruments at LCLS have provided the tools for previously impossible experiments. The study of faster scale processes has provided significant insight in various fields of physical studies. Some of these studies are presented in Section 6.

# 6 Some Interesting Research at LCLS

The research done at LCLS since its operations began in 2009 demonstrate the usefulness of the high intensity monochromatic coherent beam and ultrashort time pulse. Here, I present some of the recent published work conducted at LCLS.

## 6.1 X-ray crystallography of mosquito insecticide [8]

A naturally occurring (produced by bacteria) paracrystalline larvicide called BinAB is used around the world as an insecticide to combat mosquito-borne diseases. The crystals are small, around 50 unit cells per edge, so usual X-ray crystallography measurements are not possible. But by understanding the structure of BinAB, it could be adapted to be more effective against certain types of mosquitos that transmit illnesses such as dengue fever and the Zika virus [8].

The high intensity of photons and small beam divergence were required to measure the crystals, but X-rays would also damage them. So the fast pulses allow for detailed structural data collection before damage is incurred [8].

## 6.2 Process of water splitting and $O_2$ formation in photosynthesis [9]

This study involved structure studies of photosystem II, a pretein complex in plants, algae, and cyanobacteria that has released most of the $O_2$ in our atmosphere. The mechanism behind the splitting of water and subsequent formation of the $O-O$ bond is not well-understood since it is difficult to duplicate the conditions under which photosynthesis occurs naturally in a laboratory and take diffraction images on a fast enough scale to see parts of the process rather than an average over the entire process. Previous studies had to be taken in a resting state with frozen samples [9].

At LCLS, the researchers were able to take images at room temperature during the photosynthesis process. They were able to see two steps and decode the process in some detail. The eventual goal is to understand how water splitting might be used in clean energy sources. This process again required a quick measurement, with diffraction data attained before the X-rays damaged the photosystem II [9].

## 6.3 Imaging the interaction between two biomolecules [10]

Inside bacterial cells, there are RNA structures called riboswitches, which, when bound to another biomolecule, regulate the production of proteins. This kind of ”switch” behavior allows a way to turn on and off protein production. Since the LCLS beam can measure small nanosized objects and make the measurement before X-ray damage is incurred, scientists were able to take snapshots of the interaction at specific time intervals. They observed a sudden change in shape of the riboswitches (and the crystals) as the second biomolecule, in this case adenine, bound to it. This change occurred much faster than it was previously thought to do [10].

## 6.4 DNA protecting itself from UV light [11]

The molecules that make up DNA tend to absorb the UV light present from sunlight very strongly. With previous knowledge of molecules and radiation, scientists thought that this absorption should result in the deactivation of the molecules and essentially the destruction of DNA under normal outdoor conditions, but clearly that is not the case most of the time. LCLS measurements were used to measure how thymine, one of the molecules in DNA, responds to a short pulse of UV radiation. Following the UV pulse they were able to use X-ray pulses at set time intervals to measure thymine’s structure. What they found was that the UV light stretched a single chemical bond, which then relaxed within 200 fs by transferring energy to other bonds and setting off vibrations throughout the molecule. This resulted in the dissipation of the energy harmlessly as heat rather than a destroyed bond. Dynamics on the scale of 200 fs would be very difficult to measure in a synchrotron source with longer pulses [11].

### 6.5 All-optical switching imaging [12]

All-optical switching is a phenomenon where circularly polarized light can be used to switch the magnetization of certain combinations of materials such as FeGdCo or CoTb or CoPt. It was of great interest in the magnetic community because the magnetic regions are able to switch much faster than they do in other phenomena used in technology, such as with field-assisted or heat-assisted magnetic recording. In this experiment, scientists directed ultrafast pulses of visible light at a sample and then measured X-ray scattering with X-ray pulses to study the evolution of the switching process. They found that the magnetization of these regions was switched up to 1000 times faster than the switching in current technology. They also were able to study small regions within the visible laser beam and view different dynamics on the nanoscale, which affects the switching process radically [12].

### 6.6 Charge-spin-lattice interactions [4, 13]

A very popular area of research in condensed matter is in studies of charge-spin-lattice interactions. There seem to be numerous mechanisms driving the interactions of electrons with nuclei and the coupling of electrons and phonons. This plays a role in solar cell conversion, superconductors, topological insulators, etc.

Lead telluride is a thermoelectric material: it generates an electric voltage when it has a thermal gradient across it or generates a thermal gradient when an electrical voltage it has an electric voltage applied across two ends. This is a property that can be exploited to recover lost heat energy as electrical energy. So naturally, we would want to study how electrons and phonons interact in these materials and adapt their use for real applications. Through pump-probe measurements, scientists found at LCLS that a pulse of light is able to excite particular electronic states through electron-phonon coupling and probe how the long-range electron forces impacted instability in lead telluride's structure and how this impacted electron-phonon coupling [13].

Epitaxial chromium is an antiferromagnet that exhibits a stable spin density wave, charge density wave, and strain wave that are all interconnected, which makes it a good system for studying charge-spin-lattice interactions. We wanted to determine how an optical laser pump pulse would affect these waves, so we used X-ray pulses following the laser pulse at LCLS. Usually, the transfer of energy is thought to immediately decrease order in a system and decouple the charges, spins, and lattice. In Cr, however, we were able to actually enhance the order with much faster than expected recoupling of the spins and charges with the lattice. This could open a new avenue for enhancement of order in materials [4].

## 7 Conclusion

Prior to 2009, synchrotron facilities were the primary X-ray sources for studies of matter. However, with the successful completion of the Linac Coherent Light Source (LCLS), the world's first X-ray free-electron laser, we now have a much more powerful tool that has enabled study of different phenomena. The key piece of the free-electron laser that provides the X-ray beam characteristics

we want is the undulator, the double series of alternating dipole magnets between which the electrons travel. The electrons have a very small deflection, but they follow a path that is sinusoidal to first order. As they travel, they emit radiation tangentially to their path, so the small deflection ensures a very narrow cone of radiation. The electron bunches are also modulated in an orderly way because of the alternating magnetic field and the field from other electrons and radiation (the high total power results from the coherence of the radiation fields from electrons in the microbunches and the small divergence of the beam and narrow spectrum results from the coherence of the radiation fields from all the microbunches within the coherence length [1]). At the end of the line, we achieve high intensity monochromatic coherent X-rays.

LCLS has seven instruments with various experimental functions for studies. It has been a resource into numerous phenomena such as how water splits to form oxygen and the interaction of molecules. The demand for use of facilities like LCLS is very high. It is unlikely that we will see this demand lower any time soon, as research on this scale has shown varied interesting behavior and there is a huge range of materials which could be studied.

# References


[1] Schmüser, P., M. Dohlus, J. Rossbach, and C. Behrens. *Free-Electron Lasers in the Ultraviolet and X-ray Regime: Physical Principles, Experimental Results, Technical Realization*. (Springer International Publishing, New York, 2014).

[2] Als-Nielson, J. and D. McMorrow. *Methods of Modern X-ray Physics*. (A. John Wiley & Sons, Chichester, United Kingdom, 2011).

[3] Tanaka, H., M. Yabashi, et al. *Nature Photonics Lett.* **6**, 540 (2012).

[4] Singer, A., S. K. K. Patel, et al. *Phys. Rev. Lett.* **117**, 056401 (2016).

[5] Emma, P., R. Akre, et al. *Nature Photonics Lett.* **4**, 641 (2010).

[6] Emma, P., K. Bane, et al. *Phys. Rev. Lett.* **92**, 074801 (2004).

[7] "Instruments of LCLS."
<https://portal.slac.stanford.edu/sites/lcls_public/instruments/Pages/default.aspx>

[8] Colletier, J. P., M. R. Sawaya, et al. *Nature.* **539**, 43 (2016).

[9] Young, I. D., M. Ibrahim, et al. *Nature Lett.* (2016).

[10] Stagno, J. R., Y. Liu, et al. *Nature Lett.* (2016).

[11] McFarland, B. K., J. P. Farrell, et al. *Nature Comm.* (2014).

[12] Graves, C. E., A. H. Reid, et al. *Nature Materials.* **12**, 293 (2013).

[13] Jiang, M. P., M. Trigo, et al. *Nature Comm.* (2016).